JACS
JOURNAL OF THE AMERICAN CHEMICAL SOCIETY

Communication

pubs.acs.org/JACS

Historical Pigment Exhibiting Ammonia Gas Capture beyond Standard Adsorbents with Adsorption Sites of Two Kinds

Akira Takahashi,[†,‡] Hisashi Tanaka,[†] Durga Parajuli,[†] Tohru Nakamura,[†] Kimitaka Minami,[†] Yutaka Sugiyama,[†] Yukiya Hakuta,[†] Shin-ichi Ohkoshi,[‡] and Tohru Kawamoto*[,†]

[†]Nanomaterials Research Institute, National Institute of Advanced Industrial Science and Technology (AIST), 1-1-1 Higashi, Tsukuba 305-8565, Japan

[‡]Department of Chemistry, School of Science, The University of Tokyo, 7-3-1 Hongo, Bunkyo-ku, Tokyo 113-0033, Japan

Supporting Information

ABSTRACT: Prussian blue is a historical pigment synthesized for the first time at the beginning of 18th century. Here we demonstrate that the historical pigment exhibits surprising adsorption properties of gaseous ammonia. Prussian blue shows 12.5 mmol/g of ammonia capacity at 0.1 MPa, whereas standard ammonia adsorbents show only 5.08−11.3 mmol/g. Dense adsorption was also observed for trace contamination in atmosphere. Results also show higher adsorption by Prussian blue analogues with the optimization of chemical composition. The respective capacities of cobalt hexacyanocobaltate (CoHCC) and copper hexacyanoferrate (CuHCF) were raised to 21.9 and 20.2 mmol/g, the highest value among the recyclable adsorbents. Also, CoHCC showed repeated adsorption in vacuum. CuHCF showed regeneration by acid washing. The chemical state of the adsorbed ammonia depends on the presence of the water in atmosphere: NH_3, which was stored as in the dehydrated case, was converted into NH_4^+ in the hydrated case.

The history of Prussian blue is quite long and well documented. In the 18th century, new pigments were invented and older ones were augmented for painting.[1] They were used widely by various painters such as Vincent Willem van Gogh and Hokusai Katsushika.[2] Since the 19th century, *in situ* photosynthesis of Prussian blue on paper has been used as a photographic method: *cyanotype*.[3] During the 20th and 21st centuries, new functionalities of Prussian blue and its analogues have been found one after another, e.g., radioactive Cs adsorbent,[4,5] electrochromism for smart window,[6,7] room temperature magnetism,[8] photomagnetism,[9−11] and utility for electrodes in Na-ion batteries.[12] For these new functionalities, the crystalline subnanometer cavity network plays a crucial role. The cavity network is a special feature of the open framework material with coordination bonding.[13−16] For their cavity networks, storage, uptake, and separation of gases are typical applications.[17−24]

Among the gases, ammonia (NH_3) is often regarded as *the next big frontier* in public health protection.[25] Actually, NH_3 released into the air combines with NO_x or SO_x into NH_4 salt, a main component of PM2.5. Reportedly, the cost of the health risk in US by NH_3 emissions from the agricultural sector is approximately $36 billion US.[26] Another report has described that reducing NH_3 emissions is the most effective means of decreasing PM2.5.[27] Furthermore, NH_3 management is necessary for various reasons: it is severely malodorous, a candidate for hydrogen storage,[28] and negatively affected contaminant in hydrogen source for fuel cell[29] that must be reduced to less than 0.1 ppm.[30]

Our aim is to demonstrate the historical pigment and its analogues as a solution for ammonia uptake technology, even from the atmosphere, in which the ammonia concentration is quite thin, 1−20 ppbv.[31] The most important characteristic of Prussian blue is the density of coordination sites in its cavity network. The crystal structure of typical Prussian blue, $Fe[Fe(CN)_6]_{0.75}$, is shown in Figure 1a, where ammonia adsorption sites of two kinds are expected: vacancy site surrounded by six NH_3-capturing metals around an $[Fe(CN)_6]$ vacancy and interstitial sites, which are confined spaces surrounded by a cubic framework, where both NH_3 and NH_4^+ would be trapped. The respective concentrations of the vacancy sites and interstitial ones are dense in principle: 6.8 and 9.0 mmol/g. Moreover, the vacancy site concentration can be enhanced by controlling the chemical composition.

First we investigated a self-made Prussian blue sample synthesized using micromixer[32] or batch method. Its chemical composition was evaluated as $K_{0.23}Fe[Fe(CN)_6]_{0.74}$ with the lattice constant a = 1.019 nm. In addition, two Prussian blue analogues, cobalt hexacyanocobaltate (CoHCC), $Co[Co(CN)_6]_{0.60}$, and copper hexacyanoferrate (CuHCF), $Cu[Fe(CN)_6]_{0.50}$, were also tested to investigate the chemical composition effect. Both CoHCC and CuHCF have more vacancies than Prussian blue has. In fact, the respective BET surface areas were 280, 547, and 848 m^2/g, for PB, CoHCF, and CoHCC (see Figures SI5 and SI6).

Adsorption isotherms for NH_3 of Prussian blue and the analogues after sufficient dehydration are shown in Figure 1b, with the literature data for standard NH_3 adsorbents,[33] i.e., ion-exchange resin (IE, Amberlyst 15), zeolite (zeolite X13), and activated carbon (Merck and Co. Inc.), and for the recently developed adsorbent having the highest capacity.[34] The amount of ammonia adsorbed into Prussian blue at 0.1 MPa was 12.5 mmol/g, greater than that of any standard adsorbent. The

Received: March 14, 2016
Published: May 5, 2016

DOI: 10.1021/jacs.6b02721
J. Am. Chem. Soc. 2016, 138, 6376−6379

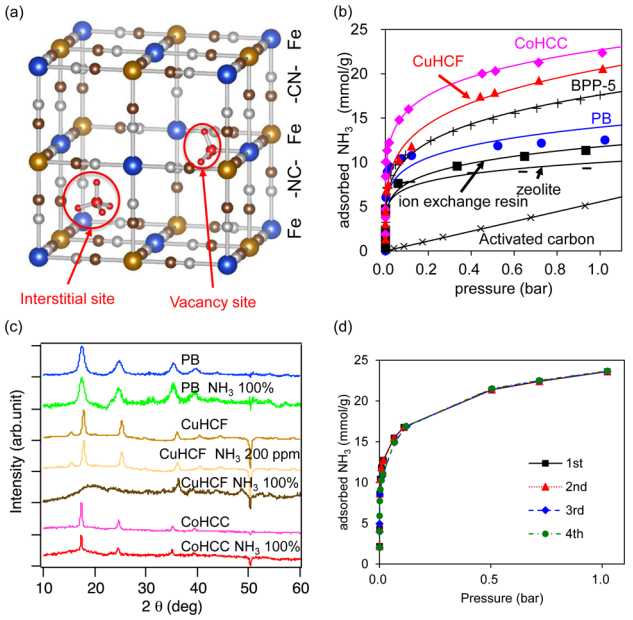

Figure 1. (a) Crystal structure of Prussian blue. (b) NH_3 adsorption isotherm of Prussian blue (PB), copper hexacyanoferrate (CuHCF), cobalt hexacyanocobaltate (CoHCC), other standard adsorbents,[33] and the recently developed adsorbent having the highest capacity.[34] Solid lines show simulation with the Freudrich model. (c) X-ray diffraction (XRD) patterns of PB, CuHCF, and CoHCC, before and after NH_3 adsorption. That of CuHCF after adsorption from the NH_3 of 200 ppmv in air is also shown. (d) NH_3 adsorption isotherms of CoHCC, the interval of obtaining each isotherm. The sample was kept at 150 °C for 24 h in vacuum.

maximum capacity was estimated as 12.4 mmol/g using the Langmuir adsorption model. We also calculated the ammonia distribution coefficient K_d, the ratio of the ammonia density in solid to that in gas, at the lower concentration of 6.23×10^{-1}–1.06×10^{1} Pa. Actually, K_d was calculated as 3.6×10^5 L(gas)/L(adsorbent), meaning that the ammonia concentration in Prussian blue is more than hundreds of thousands of times as high as that in gas phase. In addition, Prussian blue analogues having more vacancies have shown higher capacity: the respective capacities of CoHCC and CuHCF estimated using the Langmuir adsorption model were 21.9 and 20.6 mmol/g, which are the highest values among porous and open framework materials.[34−44] The adsorption rate to reach the equilibrium of CoHCC is faster than that of the IE and zeolite, as shown in SI 1.7.

During the adsorption process, Prussian blue and CoHCC were confirmed not to degrade. From X-ray diffraction (XRD) analysis results presented in Figure 1c, the crystal structures of Prussian blue and CoHCC were maintained after NH_3 adsorption. Especially, CoHCC showed adsorption−desorption processes repeatedly without any decrease of capacity, as shown in Figure 1d. The NH_3-capacity per volume of CoHCC 25.6 mol/L is highest among the adsorbents maintaining a crystal structure after the adsorption (see Figure SI3). Maintenance of the crystal structure is important for applications because the change of the crystal structure and the volume often causes degradation. For example, $Mg(NH_3)_6Cl_2$[45] expands its volume to 3.9 times by the NH_3 adsorption, although it exhibits higher NH_3 capacity.[46]

In contrast, the XRD peaks of CuHCF disappeared after NH_3 adsorption, indicating that CuHCF transformed into an amorphous material. The reason for the degradation of CuHCF would be too many $[Fe(CN)_6]$ vacancies. The XRD peaks of CuHCF remained after the use of thinner NH_3, 200 ppmv of NH_3 in air (Figure 1d), indicating that the CuHCF was not degraded by trace NH_3 adsorption.

The adsorption mechanism was confirmed from infrared (IR) spectra for Prussian blue obtained in ambient air after ammonia adsorption, implying the transformation of NH_3 into NH_4^+ with H_2O in air. As Figure 2a shows, new adsorption peaks appeared

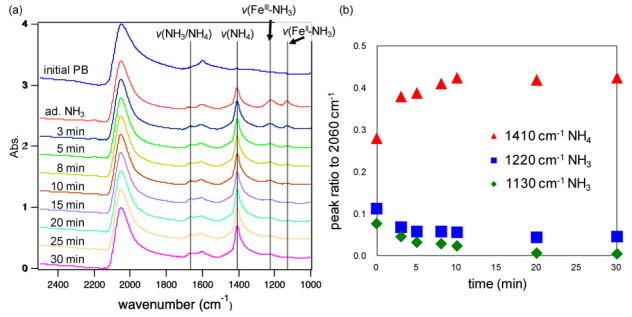

Figure 2. (a) Time variation of the FTIR peaks in ambient air after the ammonia adsorption test. (b) Time variation of the IR peak height of Prussian blue at 1410, 1220, and 1130 cm^{-1} at leaving ambient air after ammonia adsorption.

after adsorption at 1670, 1410, 1220, and 1130 cm^{-1}, respectively, corresponding to degenerate deformation (δ_d) of NH_3/NH_4^+, symmetric deformation (δ_d) of NH_4^+, δ_d of (Fe^{III}–NH_3), and δ_d of (Fe^{II}–NH_3),[47,48] indicating that some of the adsorbed ammonia exists at $[Fe(CN)_6]$ vacancy sites with coordination bonding at Fe sites and that the form of ammonia, whether NH_3 or NH_4^+, can be detected from infrared spectra.

The NH_4^+ is expected to be generated from NH_3 adsorbed in Prussian blue and H_2O in ambient air.[49] The transformation from NH_3 to NH_4^+ was confirmed by variation of the related IR peaks over time after the sample exposure to air. Figure 2b shows time variation of the ratio of the IR peak height at 1410, 1220, and 1130 cm^{-1} to 2060 cm^{-1}, where the peak of 2060 cm^{-1} corresponds to CN^- vibration in the Prussian blue framework. The peaks at 1220 and 1130 cm^{-1} corresponding to Fe−NH_3 decrease, but that at 1410 cm^{-1}, corresponding to NH_4^+, increases. Both changes seem to finish by 10 min. The result shows that the mechanism of the ammonia adsorption by Prussian blue in the presence of water resembles that of an ion-exchange resin, where adsorbed NH_3 transforms to $NH_4^+ + OH^-$ by combination with H_2O.

Even in ambient air with only approximately 15 ppbv of ammonia, the partial pressure of NH_3 is 10^{-5} kPa; Prussian blue also functions as the ammonia adsorbent. Figure 3a portrays the time variation of the IR spectrum of fresh Prussian blue when left in ambient air in our laboratory, where the concentration of ammonia in gas phase ($\rho_g(NH_x)$) was 15.1 ± 2.0 ppbv. The peak at 1410 cm^{-1} was found to increase over time. The variation of the concentration was well simulated by the pseudo-first order model. The ammonia concentration in Prussian blue was saturated with 0.30 mmol/g after approximately 30 h exposure. The IR peaks corresponding to NH_3 were not observed because more time is necessary for ammonia adsorption than for transformation from NH_3 to NH_4^+. The K_d in ambient air was estimated as 6.8×10^8 L(gas)/L(adsorbent), more than thousands of times higher than the value for pure NH_3 gas described above. Enhancement of the NH_3 adsorption ability in

DOI: 10.1021/jacs.6b02721
J. Am. Chem. Soc. 2016, 138, 6376−6379

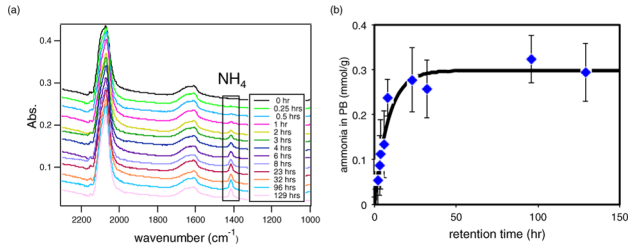

Figure 3. (a) Time dependence of FTIR spectra of Prussian blue while maintaining ambient air in laboratory. (b) Time dependence of FTIR absorption peak ratios of 1410−2060 cm^{-1}.

ambient air is expected to be caused by the stabilization of NH_3 into the NH_4^+ in the combination with H_2O in Prussian blue. The adsorption speed of PB is than that of IE and zeolite in the NH_3 adsorption process. Details are presented in SI 1.13 and Figure SI3.

To confirm the availability for the practical application of trace NH_3 uptake, we evaluated NH_3 removal from air using a column filled with Prussian blue or its analogues, demonstrating that all of them exhibited sufficient performance. Ambient air with trace ammonia gas, $\rho_g(NH_3)$ approximately 1 ppmv, was passed through the column with approximately 2 ms of contact time. Results show that 96%, 90%, and 95% of NH_3 were removed respectively from the air by Prussian blue, CuHCF, and CoHCC (Figure SI9). For all cases, $\rho_g(NH_3)$ after passage through the column is less than 0.1 ppmv, the human detection threshold[50] and also the upper limit of impurity g-NH_3 in fuel hydrogen by ISO regulations.[30] This result shows sufficiently prompt adsorption for realistic use.

Reusability was also confirmed. Actually, CuHCF exhibited good reusability for trace NH_3 uptake by desorption with acid washing. Figure 4 shows ammonia desorption from CuHCF

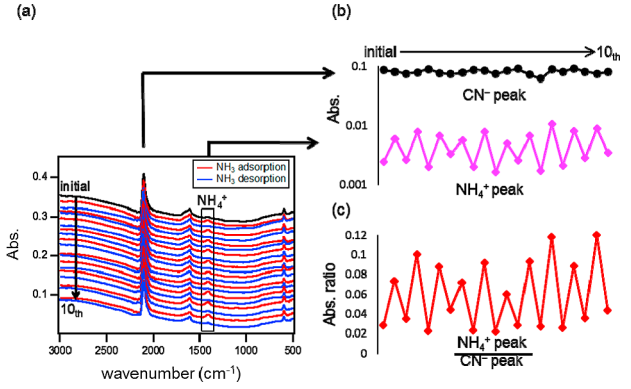

Figure 4. Cyclic processes of ammonia adsorption and desorption of CuHCF: (a) IR spectra in each process of adsorption and desorption; (b) change of the peak height corresponding to CN^- (2060 cm^{-1}) and NH_4^+ (1410 cm^{-1}); and (c) ratio of the peak height of CN^- to NH_4^+.

achieved by rinsing with sulfonic acid, as verified with IR spectra. During the 10 sequential processes of adsorption and desorption, the IR peak corresponding to NH_4^+ clearly appears by contact with ammonia gas and disappears by rinsing with sulfuric acid. CoHCC shows reusability with a half of its capacity, although Prussian blue showed difficult desorption (Figure SI10).

Adsorption sites of these two types depending on the presence of water become beneficial for each application. When the material is used for NH_3 storage, the dehydrated situation, the material adsorbs NH_3 as it is. However, for the adsorbent for trace NH_3 in atmosphere, the hydrated case, ammonia is adsorbed as NH_4^+ with larger K_d, indicating avoidance of the rerelease of adsorbed ammonia.

In summary, we found surprising ammonia adsorption properties of Prussian blue, adsorbing ammonia even at trace levels from ambient air. Over a long period, many pictures and photographs using Prussian blue might capture ammonia from the atmosphere. Results show that its adsorption performance can be improved by crystal engineering, metal substitution, and control of its vacancy density. The chemical state of the adsorbed ammonia depends on the presence of water, an advantage for the utilization for each application. Therefore, Prussian blue and its analogues are expected to supply effective ammonia management technologies.

■ ASSOCIATED CONTENT

Supporting Information

The Supporting Information is available free of charge on the ACS Publications website at DOI: 10.1021/jacs.6b02721.

Methods for synthesis, film fabrication, adsorption isotherm, ammonia concentration in atmosphere, ammonia concentration in Prussian blue, cycle test, and column test. Characterization, crystal structure during adsorption process, ammonia adsorption isotherm in low pressure, time required for equilibrium, adsorption enthalpy, and BET specific surface area. Figures: SEM images, isotherm in lower pressure, K_d variation in the column test, capacity comparisons with other adsorbents, rough estimation of enthalpy, BET evaluation, calibration line for the evaluation of NH_4^+ concentration in by FTIR, and details of column test and regeneration test (PDF)

■ AUTHOR INFORMATION

Corresponding Author

*tohru.kawamoto@aist.go.jp

Notes

The authors declare no competing financial interest.

■ ACKNOWLEDGMENTS

The present research was partially supported by JSPS KAKENHI Grant Number 15H05697.

■ REFERENCES

(1) Kraft, A. *Bull. Hist. Chem.* **2008**, *33* (2), 61.
(2) McCouat, P. Prussian Blue and Its Partner in Crime. Journal of Art in Society. http://www.artinsociety.com/prussian-blue-and-its-partner-in-crime.html (accessed Sep 6, 2015).
(3) Ware, M. Cyanotype: The History, Science and Art of Photographic Printing in Prussian Blue. In *Science Museum*, 1999.
(4) Haas, A. P. *Sep. Sci. Technol.* **1993**, *28*, 2479.
(5) Liu, X.; Chen, G. R.; Lee, D. J.; Kawamoto, T.; Tanaka, H.; Chen, M. L.; Luo, Y. K. *Bioresour. Technol.* **2014**, *160*, 142.
(6) Neff, V. D. *J. Electrochem. Soc.* **1978**, *125* (6), 886.
(7) Kraft, A.; Rottmann, M. *Sol. Energy Mater. Sol. Cells* **2009**, *93* (12), 2088.
(8) Ferlay, S.; Mallah, T.; Ouahès, R.; Veillet, P.; Verdaguer, M. *Nature* **1995**, *378* (6558), 701.
(9) Sato, O.; Iyoda, T.; Fujishima, A.; Hashimoto, K. *Science* **1996**, *272* (5262), 704.
(10) Escax, V.; Bleuzen, a.; Cartier dit Moulin, C.; Villain, F.; Goujon, a.; Varret, F.; Verdaguer, M. *J. Am. Chem. Soc.* **2001**, *123* (50), 12536.
(11) Tokoro, H.; Matsuda, T.; Nuida, T.; Moritomo, Y.; Ohoyama, K.; Dangui, E. D. L.; Boukheddaden, K.; Ohkoshi, S. *Chem. Mater.* **2008**, *20* (2), 423.

DOI: 10.1021/jacs.6b02721
J. Am. Chem. Soc. 2016, 138, 6376−6379

(12) Pasta, M.; Wessells, C. D.; Liu, N.; Nelson, J.; McDowell, M. T.; Huggins, R. a; Toney, M. F.; Cui, Y. *Nat. Commun.* **2014**, *5*, 3007.
(13) Kondo, M.; Yoshitomi, T.; Matsuzaka, H.; Kitagawa, S.; Seki, K. *Angew. Chem., Int. Ed. Engl.* **1997**, *36* (16), 1725.
(14) Park, K. S.; Ni, Z.; Côté, A. P.; Choi, J. Y.; Huang, R.; Uribe-Romo, F. J.; Chae, H. K.; O'Keeffe, M.; Yaghi, O. M. *Proc. Natl. Acad. Sci. U. S. A.* **2006**, *103* (27), 10186.
(15) Kitagawa, S.; Kitaura, R.; Noro, S. *Angew. Chem., Int. Ed.* **2004**, *43* (18), 2334.
(16) Murray, L. J.; Dincă, M.; Long, J. R. *Chem. Soc. Rev.* **2009**, *38* (5), 1294.
(17) Kaye, S. S.; Long, J. R. *J. Am. Chem. Soc.* **2005**, *127* (18), 6506.
(18) Thallapally, P. K.; Motkuri, R. K.; Fernandez, C. A.; McGrail, B. P.; Behrooz, G. S. *Inorg. Chem.* **2010**, *49* (11), 4909.
(19) Reguera, L.; Krap, C. P.; Balmaseda, J.; Reguera, E. *J. Phys. Chem. C* **2008**, *112* (40), 15893.
(20) Ogilvie, S. H.; Duyker, S. G.; Southon, P. D.; Peterson, V. K.; Kepert, C. J. *Chem. Commun. (Cambridge, U. K.)* **2013**, *49* (82), 9404.
(21) Karadas, F.; El-Faki, H.; Deniz, E.; Yavuz, C. T.; Aparicio, S.; Atilhan, M. *Microporous Mesoporous Mater.* **2012**, *162*, 91.
(22) Barea, E.; Montoro, C.; Navarro, J. A. R. *Chem. Soc. Rev.* **2014**, *43* (16), 5419.
(23) Férey, G. *Chem. Soc. Rev.* **2008**, *37* (1), 191.
(24) Yaghi, O. M.; O'Keeffe, M.; Ockwig, N. W.; Chae, H. K.; Eddaoudi, M.; Kim, J. *Nature* **2003**, *423* (6941), 705.
(25) Stokstad, E. *Science* **2014**, *343* (6168), 238.
(26) Paulot, F.; Jacob, D. J. *Environ. Sci. Technol.* **2014**, *48* (2), 903.
(27) Megaritis, A. G.; Fountoukis, C.; Charalampidis, P. E.; Pilinis, C.; Pandis, S. N. *Atmos. Chem. Phys.* **2013**, *13* (6), 3423.
(28) Klerke, A.; Christensen, C. H.; Nørskov, J. K.; Vegge, T. *J. Mater. Chem.* **2008**, *18* (20), 2304.
(29) Cheng, X.; Shi, Z.; Glass, N.; Zhang, L.; Zhang, J.; Song, D.; Liu, Z.-S.; Wang, H.; Shen, J. *J. Power Sources* **2007**, *165* (2), 739.
(30) ISO14687-2, 2012.
(31) Carmichael, G. R.; Ferm, M.; Thongboonchoo, N.; Woo, J.-H.; Chan, L.; Murano, K.; Viet, P. H.; Mossberg, C.; Bala, R.; Boonjawat, J.; Upatum, P.; Mohan, M.; Adhikary, S. P.; Shrestha, A. B.; Pienaar, J.; Brunke, E. B.; Chen, T.; Jie, T.; Guoan, D.; Peng, L. C.; Dhiharto, S.; Harjanto, H.; Jose, A. M.; Kimani, W.; Kirouane, A.; Lacaux, J.-P.; Richard, S.; Barturen, O.; Cerda, J. C.; Athayde, A.; Tavares, T.; Cotrina, J. S.; Bilici, E. *Atmos. Environ.* **2003**, *37* (9−10), 1293.
(32) Takahashi, A.; Minami, N.; Tanaka, H.; Sue, K.; Minami, K.; Parajuli, D.; Lee, K.-M.; Ohkoshi, S.; Kurihara, M.; Kawamoto, T. *Green Chem.* **2015**, *17* (8), 4228.
(33) Helminen, J.; Helenius, J.; Paatero, E.; Turunen, I. *J. Chem. Eng. Data* **2001**, *46* (2), 391.
(34) Van Humbeck, J. F.; McDonald, T. M.; Jing, X.; Wiers, B. M.; Zhu, G.; Long, J. R. *J. Am. Chem. Soc.* **2014**, *136* (6), 2432.
(35) Kajiwara, T.; Higuchi, M.; Watanabe, D.; Higashimura, H.; Yamada, T.; Kitagawa, H. *Chem. - Eur. J.* **2014**, *20* (47), 15611.
(36) Doonan, C. J.; Tranchemontagne, D. J.; Glover, T. G.; Hunt, J. R.; Yaghi, O. M. *Nat. Chem.* **2010**, *2* (3), 235.
(37) Saha, D.; Deng, S. *J. Colloid Interface Sci.* **2010**, *348* (2), 615.
(38) Petit, C.; Wrabetz, S.; Bandosz, T. J. *J. Mater. Chem.* **2012**, *22* (40), 21443.
(39) Grant Glover, T.; Peterson, G. W.; Schindler, B. J.; Britt, D.; Yaghi, O. *Chem. Eng. Sci.* **2011**, *66* (2), 163.
(40) Furtado, A. M. B.; Liu, J.; Wang, Y.; LeVan, M. D. *J. Mater. Chem.* **2011**, *21* (18), 6698.
(41) Shiralkar, V.; Kulkarni, S. *J. Colloid Interface Sci.* **1985**, *108* (1), 1.
(42) Saha, D.; Deng, S. *J. Colloid Interface Sci.* **2010**, *345* (2), 402.
(43) DeCoste, J. B.; Peterson, G. W.; Schindler, B. J.; Killops, K. L.; Browe, M. A.; Mahle, J. J. *J. Mater. Chem. A* **2013**, *1* (38), 11922.
(44) Bernal, M. P.; Lopez-Real, J. M. *Bioresour. Technol.* **1993**, *43* (1), 27.
(45) Liu, C. Y.; Aika, K. *Ind. Eng. Chem. Res.* **2004**, *43* (23), 7484.
(46) Jacobsen, H. S.; Hansen, H. A.; Andreasen, J. W.; Shi, Q.; Andreasen, A.; Feidenhans'l, R.; Nielsen, M. M.; Ståhl, K.; Vegge, T. *Chem. Phys. Lett.* **2007**, *441* (4−6), 255.
(47) Nakamoto, K. *Infrared and Raman Spectra of Inorganic and Coordination Compounds: Part B: Applications in Coordination, Organometallic, and Bioinorganic Chemistry*, 6th ed.; John Wiley & Sons, Inc, 2008.
(48) Schimek, G. L.; Kolis, J. W.; Long, G. J. *Chem. Mater.* **1997**, *9* (12), 2776.
(49) Balmaseda, J.; Reguera, E.; Fernández, J.; Gordillo, A.; Yee-Madeira, H. *J. Phys. Chem. Solids* **2003**, *64* (4), 685.
(50) Nakanishi, M. Measures against Offensive Odors. http://www.env.go.jp/en/focus/docs/files/20130118-61.pdf (accessed Oct 18, 2015).

DOI: 10.1021/jacs.6b02721
J. Am. Chem. Soc. 2016, 138, 6376−6379